Development of ^{64}Cu-NOTA-Trastuzumab for HER2 Targeting: A Radiopharmaceutical with Improved Pharmacokinetics for Human Studies

Sang-Keun Woo*[1], Su Jin Jang*[1], Min-Jung Seo[1], Ju Hui Park[1], Byoung Soo Kim[1], Eun Jung Kim[1], Yong Jin Lee[1], Tae Sup Lee[1], Gwang Il An[1], In Ho Song[1], Youngho Seo[2], Kwang Il Kim†[1], and Joo Hyun Kang†[1]

[1]*Division of RI–Convergence Research, Korea Institute of Radiological and Medical Sciences, Seoul, Republic of Korea; and*
[2]*Department of Radiology, University of California San Francisco School of Medicine, San Francisco, California*

See an invited perspective on this article on page 23.

The purpose of this study was to develop ^{64}Cu-labeled trastuzumab with improved pharmacokinetics for human epidermal growth factor receptor 2 (HER2). **Methods:** Trastuzumab was conjugated with SCN-Bn-NOTA and radiolabeled with ^{64}Cu. Serum stability and immunoreactivity of ^{64}Cu-NOTA-trastuzumab were tested. Small-animal PET imaging and biodistribution studies were performed in a HER2-positive breast cancer xenograft model (BT-474). The internal dosimetry for experimental animals was determined using the image-based approach with the Monte Carlo N-particle code. **Results:** ^{64}Cu-NOTA-trastuzumab was prepared with high radiolabeling yield and radiochemical purity (>98%) and showed high stability in serum and good immunoreactivity. Uptake of ^{64}Cu-NOTA-trastuzumab was highest at 48 h after injection as determined by PET imaging and biodistribution results in BT-474 tumors. The blood radioactivity concentrations of ^{64}Cu-NOTA-trastuzumab decreased biexponentially with time in both mice with and mice without BT-474 tumor xenografts. The calculated absorbed dose of ^{64}Cu-NOTA-trastuzumab was 0.048 mGy/MBq for the heart, 0.079 mGy/MBq for the liver, and 0.047 mGy/MBq for the spleen. **Conclusion:** ^{64}Cu-NOTA-trastuzumab was effectively targeted to the HER2-expressing tumor in vitro and in vivo, and it exhibited a relatively low absorbed dose due to a short residence time. Therefore, ^{64}Cu-NOTA-trastuzumab could be applied to select the right patients and right timing for HER2 therapy, to monitor the treatment response after HER2-targeted therapy, and to detect distal or metastatic spread.

Key Words: HER2; ^{64}Cu-NOTA-trastuzumab; absorbed dose; patient selection; treatment response

J Nucl Med 2019; 60:26–33
DOI: 10.2967/jnumed.118.210294

Human epidermal growth factor receptor 2 (HER2), a transmembrane receptor tyrosine kinase 2, is overexpressed in gastric cancer, ovary cancer, prostate cancer, and lung cancer, as well as breast cancer. HER2 is a proven therapeutic target for breast and gastric cancer (*1,2*); it is highly expressed in 15%–20% of breast cancers, and HER2-positive characteristics are associated with more aggressive growth, worse prognosis, greater possibility of recurrence, and shorter survival than for HER2-negative breast cancer (*3*). Several anti-HER2 agents have been successfully developed and applied to HER2-positive breast cancer, including trastuzumab and pertuzumab as antibody therapeutics and lapatinib and neratinib as HER2 tyrosine kinase inhibitors (*4*).

Trastuzumab is a humanized monoclonal antibody that targets the extracellular portion of HER2 and is the first HER2-targeted agent approved by the U.S. Food and Drug Administration for treating both early-stage and metastatic HER2-overexpressing breast cancer (*5*). For effective treatment with HER2-targeting agents, it is important to validate HER2 expression in the primary tumor and metastatic sites. Although there is a routine examination of HER2 expression using immunohistochemistry or fluorescence in situ hybridization, technical problems can arise when lesions are not easily accessible by core-needle biopsy, including whole-body metastasis. In addition, HER2 expression can vary during the course of the disease and even among tumor lesions in the same patient. Thus, a PET imaging probe using radiolabeled antibodies based on Food and Drug Administration–approved trastuzumab has been studied for the noninvasive evaluation of HER2 expression (*6*). Additionally, a molecular imaging technique with radiolabeled trastuzumab can be applied to select the right timing for HER2 therapy, to monitor the treatment response after HER2-targeted therapy, and to detect distal or metastatic spread. For this purpose, several PET or SPECT agents with trastuzumab using ^{64}Cu, ^{124}I, ^{111}In, and ^{89}Zr were developed (*7–10*). Especially, ^{64}Cu-DOTA-trastuzumab using DOTA as a bifunctional chelator was developed and applied to clinical studies for individualizing treatment of HER2-positive metastatic tumors and HER2-positive breast cancer (*11–15*).

In addition, a properly designed antibody–chelate immunoconjugate could serve as a therapeutic agent or imaging probe by introducing a radioisotope. ^{90}Y-labeled ibritumomab tiuxetan (Zevalin; Spectrum Pharmaceuticals) is a radioimmunotherapy pharmaceutical for recurrent and resistant forms of low-grade follicular B-cell non-Hodgkin lymphoma. SPECT imaging with ^{111}In-ibritumomab tiuxetan was performed to select the right patients for ^{90}Y-ibritumomab tiuxetan treatment (*16*).

Because antibody molecules are labile to heat, pH, and agents such as salt and detergents, forming antibody–chelator conjugates before introducing the radioisotope is a proper strategy for preparation and quality control of radiopharmaceuticals with antibody

Received Feb. 21, 2018; revision accepted May 14, 2018.
For correspondence or reprints contact: Joo Hyun Kang, Division of RI–Convergence Research, Korea Institute of Radiological and Medical Sciences 75, Nowon-ro, Nowon-gu, Seoul, Republic of Korea.
E-mail: kang2325@kirams.re.kr
*Contributed equally to this work.
†Contributed equally to this work.
Published online May 18, 2018.

molecules. In particular, an appropriately structured antibody–chelator conjugate could be applicable for therapeutic or imaging purposes by introducing a metallic therapeutic or imaging radioisotope such as ^{90}Y-labeled ibritumomab tiuxetan or ^{111}In-labeled ibritumomab tiuxetan. ^{64}Cu, with a half-life of 12.7 h, is the most widely studied PET radioisotope. It can be produced via the ^{64}Ni(p,n)^{64}Cu reaction using a cyclotron in a carrier-free state (*17*). The optimal structure of the antibody–chelator conjugate for ^{64}Cu could be used for therapeutic β-emitter ^{67}Cu (half-life, 2.58 d) as a pair of radioisotopes of ^{64}Cu (*18*). Because ^{64}Cu-radiolabeled complexes with improved stability have been reported with NOTA derivatives (*19*), we introduced NOTA as a chelator for ^{64}Cu labeling into trastuzumab antibody to provide the more favorable pharmacokinetic of ^{64}Cu-labeled trastuzumab than that of DOTA as a chelator. Moreover, we can predict the internal absorbed radiation dose of ^{67}Cu-labeled antibody using ^{64}Cu-labeled antibody (*20,21*), which is a powerful advantage for ^{64}Cu/^{67}Cu-labeled antibody development as a PET probe or therapeutic agent (Supplemental Fig. 1; supplemental materials are available at http://jnm.snmjournals.org).

The purpose of this study was to develop ^{64}Cu-labeled trastuzumab using NOTA as a chelator with improved pharmacokinetics for HER2 and to evaluate the pharmacokinetic characteristics and image-based absorbed dose of ^{64}Cu-NOTA-trastuzumab for human study.

MATERIALS AND METHODS

Preparation of ^{64}Cu-NOTA-Trastuzumab

Trastuzumab (Herceptin; Roche) was buffer-exchanged and concentrated to 10 mg/mL in 0.1 M 4-(2-hydroxyethyl)-1-piperazineethanesulfonic acid (HEPES) buffer, pH 8.5, using Vivaspin-20 centrifugal concentrators (Sartorius). A 20-fold molar excess of *p*-SCN-Bn-NOTA (Macrocyclics) in 100% ethanol was added to the antibody in 0.1 M HEPES buffer. After incubation at 4°C overnight for conjugation, the reaction mixture was purified and concentrated to 5 mg/mL with 0.1 M ammonium acetate buffer, pH 6, using Vivaspin-20. Mass spectrometry was performed to determine the number of chelates per antibody.

The immunoconjugate (NOTA-trastuzumab) was radiolabeled with ^{64}Cu produced at KIRAMS by 50-MeV cyclotron irradiation (*22*). $^{64}CuCl_2$ (74 MBq) was added to 1 mg of NOTA-trastuzumab. The reaction mixtures were incubated at room temperature for 1 h with constant agitation followed by testing of the radiolabeling yield and purity by instant thin-layer chromatography using silica gel paper (Agilent Technologies) as the stationary phase and 0.1 M ammonium acetate buffer, pH 6, with 50 mM ethylenediaminetetraacetic acid as the mobile phase.

Stability Testing of ^{64}Cu-NOTA-Trastuzumab

We tested the in vitro serum stability of the radiolabeled antibodies using instant thin-layer chromatography as described above by incubating 100 μL (7.4 MBq) of radiolabeled antibodies in 100 μL of fresh human serum, mouse serum, and phosphate-buffered saline at 37°C for 1, 4, 6, 12, 24, and 48 h. To determine the shelf life at 4°C, we measured the radiochemical purity of ^{64}Cu-NOTA-trastuzumab immediately and 24 h after labeling.

Cell Culture and Animals

The HER2-positive cell line, BT-474, was obtained from the American Type Culture Collection and was grown in RPMI-1640 medium (Corning) supplemented with 10% heat-inactivated fetal bovine serum (Gibco) and antibiotics (penicillin G, 100 units/mL, and streptomycin, 10 μg/mL; Gibco) at 37°C in a humidified 5% CO_2 atmosphere.

All animal experiments were carried out under a protocol approved by the KIRAMS Institutional Animal Care and Use Committee (kirams2016-0097). Six-week-old female BALB/c nude mice were purchased from NARA Biotech. Ectopic or orthotopic xenografts were produced by implanting 1×10^7 BT-474 cells in right flank skin or mammary fat pad, respectively.

Immunoreactivity

In vitro immunoreactivity of the ^{64}Cu-NOTA-trastuzumab samples was determined using specific radioactive cell-binding assays following procedures modified from Lindmo et al. (*23*). Briefly, 7 different serial dilutions of BT-474 cells starting at 6×10^6 cells/500 μL were prepared in phosphate-buffered saline (pH 7.4) supplemented with 1% bovine serum albumin. ^{64}Cu-NOTA-trastuzumab (200 ng) was added to each tube ($n = 3$) and incubated for 3 h at 4°C. Cells were collected by centrifugation, resuspended, and washed twice with cold phosphate-buffered saline before the ^{64}Cu-activity associated with the cell pellet was counted. Competitive inhibition (blocking) studies were conducted using the same procedure but with the addition of non-radiolabeled trastuzumab (A >1,000-fold excess of monoclonal antibody; 210 μg) to the ^{64}Cu-NOTA-trastuzumab solutions. After incubation, the radioactivity of tubes was read using a 1480 Wizard γ-counter (PerkinElmer). The immunoreactive fraction was determined by performing a linear regression analysis on a double inverse plot of (total/bound) activity versus normalized cell concentration. The immunoreactive fraction was obtained from the inverse of the intercept on the plot.

Autoradiography and Immunohistochemistry

Immediately after PET scanning, the mice were killed and tumor tissues were removed and frozen in FSC22 tissue-freezing medium (Leica Biosystems). After the tissues had decayed for 48 h, we obtained sections with a thickness of 20 μm using a CM1800 cryostat microtome (Leica Instruments) and exposed them on imaging plates for 24 h. We scanned the plates with BAS-5000 (Fujifilm). We quantified image intensity in the region of interest as units of photostimulated luminescence per square millimeter using Fujifilm Multi Gauge software, version 3.0 (Fujifilm).

Frozen tumor tissues were sectioned at 5 μm, incubated overnight at 4°C with anti-HER2 antibody (1:50 dilution; Cell Signaling Technology), and incubated for 30 min at room temperature with goat antirabbit IgG-horseradish peroxidase (1:200 dilution; Santa Cruz Biotechnology). We used a 3,3′-diaminobenzidine kit (DAKO) for color development and subsequently counterstained the slides with hematoxylin.

Biodistribution Study

Biodistribution studies were performed to evaluate the uptake of ^{64}Cu-NOTA-trastuzumab in normal and subcutaneous BT-474 tumor–bearing mice. At 2, 6, 24, 48, and 72 h after the intravenous administration of 3.7 MBq of ^{64}Cu-NOTA-trastuzumab, the mice were sacrificed, their organs were removed and weighed, and radioactivity was measured. Results are expressed as percentage injected dose (%ID) per gram of tissue ($n = 4$).

Pharmacokinetic Study of ^{64}Cu-NOTA-Trastuzumab in Nude Mice With or Without HER2-Positive Tumor

^{64}Cu-NOTA-trastuzumab was injected into nude mice with or without BT-474 tumor xenografts via their tail veins at 5.5–6.7 MBq (150–180 μCi)/100 μg/head ($n = 6$ each). Blood samples were collected from the retroorbital plexus into a 75-mm sodium-heparinized capillary tube at 0, 0.167, 0.5, 1, 2, 6, 24, 48, and 72 h after administration. Dosing solution (2 μL) and blood samples (30 μL) were transferred to polyethylene tubes. Radioactivity was counted by

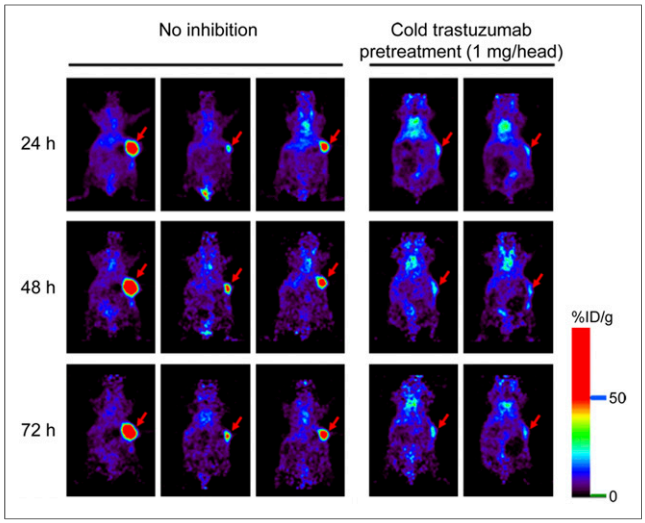

FIGURE 1. ^{64}Cu-NOTA-trastuzumab PET images in HER2-positive tumor model. Right 2 columns display PET images after cold trastuzumab pretreatment (n = 2), and left 3 show nonblocking images (n = 3). Arrows indicate BT-474 tumors.

a 1480 Wizard γ-counter. The radioactivity concentration of the blood sample was expressed as the %ID per milliliter of blood.

Pharmacokinetic parameters were estimated from the blood radioactivity concentration versus time by a noncompartmental method using the nonlinear least-squares regression program WinNonlin, version 2.0 (Pharsight).

S Value and Absorbed Dose Calculation

We used tumor and organ tissue density to determine S value. CT density and PET radioactivity were used as input data in the Monte Carlo simulation. S value and a dose map of organs and tumor were calculated using Geant4 Monte Carlo N-particle code. The S value equation is

$$S(r_{target} \leftarrow r_{source}) = \frac{k\sum y_i E_i \emptyset_i (r_{target} \leftarrow r_{source})}{m_{target}},$$

where y_i is the number of energy, E_i is the energy per radiation, and m is the mass of the target region.

The absorbed dose(D_{r_T}) was calculated according to the formula

$$D_{r_T} = A_0 \sum_i \tilde{A}_{r_j} \cdot S(r_T \leftarrow r_s),$$

where A_0 is the initial injected radioactivity, $\tilde{A}_{r_j}$is the radiotracer residence time of a source organ r_i, and $S(r_T \leftarrow r_s)$is the dose deposited in target r_T per unit of cumulated activity in source r_s. Each organ and tumor absorbed dose includes contributions from the self-dose and the cross-dose from other segmented regions (*24*).

Small-Animal PET/CT Imaging

At 1, 2, and 6 h, and 1, 2, and 3 d after the intravenous injection of 7.4 MBq of ^{64}Cu-NOTA-trastuzumab per animal, the mice were placed in a spread prone position under inhalation anesthesia (isoflurane, 2%) and imaged for 20 min with an Inveon dedicated small-animal PET/CT scanner (Siemens Healthcare; n = 3). The counting rates in the reconstructed images were converted to activity concentrations (%ID per gram of tissue). To define each organ and tumor in the mice, we acquired contrast CT data using ExiTron nano 12000 (Miltenyi Biotec). Blocking studies (n = 2) were performed to evaluate the HER2 specificity of ^{64}Cu-NOTA-trastuzumab in vivo, where each mouse in a group of two was injected with 1 mg of nonlabeled trastuzumab within 1 h before ^{64}Cu-NOTA-trastuzumab administration.

Analysis of Time–Activity Curve and Residence Time

Mouse images were acquired at 6 time points after the radiotracer administration. PET image data and CT image data were colocalized, and the PET image data were segmented for each organ and tumor to calculate time–activity curve and S value. Individual mouse CT data were segmented by referral to the contrast CT image. Tumors and organs were segmented by mean-based region-growing 3-dimensional segmentation. The time–activity curve was expressed as %ID/g. Residence times were calculated via time–activity curves of acquired region-segmented PET data.

RESULTS

Quantification of ^{64}Cu-NOTA-Trastuzumab in HER2-Positive Breast Tumor PET Images

To evaluate the potential of ^{64}Cu-NOTA-trastuzumab as a PET imaging agent for HER2 expression, we performed PET imaging in ectopic BT-474 tumor models. BT-474 tumors were clearly visible on PET images after 24 h (Fig. 1). Quantitative data obtained from region-of-interest analysis of the PET results in the nonblocking group are shown in Figure 2A. Liver uptake for ^{64}Cu-NOTA-trastuzumab was 14.64 ± 2.23, 13.23 ± 1.34, and 9.50 ± 0.32 %ID/g at 24, 48, and 72 h, respectively (n = 3). Radioactivity in the blood was 19.23 ± 4.43, 15.00 ± 2.45, and 13.03 ± 3.71 %ID/g at 24, 48, and 72 h, respectively (n = 3). Importantly, tumor uptake of ^{64}Cu-NOTA-trastuzumab accumulated and was clearly visible at 24 h, peaked at 48 h, and remained prominent over time (24.82 ± 11.16, 29.24 ± 16.45, and 28.34 ± 15.89 %ID/g at 24, 48, and 72 h, respectively; n = 3).

Administering a blocking dose of trastuzumab 1 h before ^{64}Cu-NOTA-trastuzumab injection significantly reduced tumor uptake to 6.80 ± 0.77, 6.85 ± 1.73, and 6.70 ± 0.49 %ID/g at 24, 48, and 72 h, respectively (n = 2; Fig. 2B), demonstrating that ^{64}Cu-NOTA-trastuzumab maintained the HER2 specificity of its parent

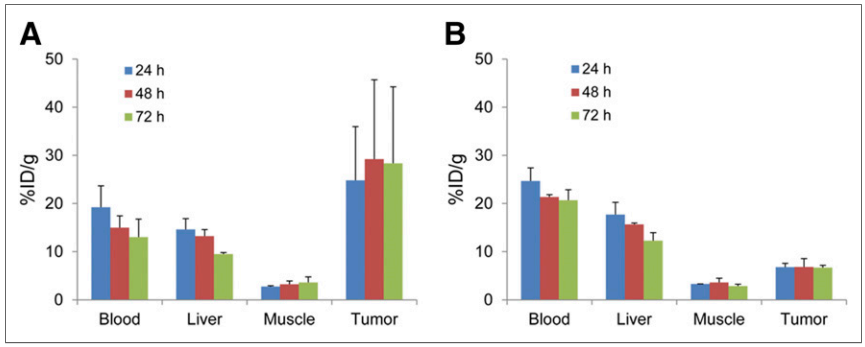

FIGURE 2. ^{64}Cu-NOTA-trastuzumab PET image quantification of nonblocking group (A) and cold trastuzumab–pretreated group (B) in HER2-positive tumor model. ^{64}Cu-NOTA-trastuzumab specificity was suggested by blocking experiments with excess of unlabeled trastuzumab.

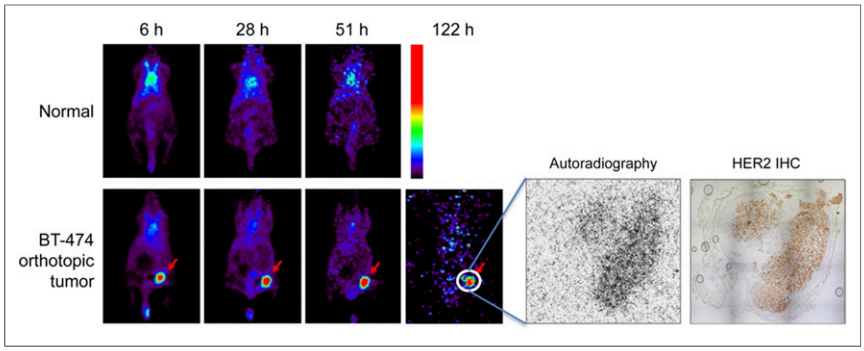

FIGURE 3. ^{64}Cu-NOTA-trastuzumab PET and immunohistochemistry in orthotopic HER2-positive BT-474 breast tumor model. Tumor uptake of ^{64}Cu-NOTA-trastuzumab was clearly visible at 6 h and peaked at 51 h, and autoradiogram of frozen section prepared from removed tumor revealed high accumulation in area where HER2-positive cells were detected by immunohistochemistry. IHC = immunohistochemistry.

antibody in vivo. Liver uptake of ^{64}Cu-NOTA-trastuzumab in the blocking group was similar to that in mice injected with ^{64}Cu-NOTA-trastuzumab alone: 17.72 ± 2.53, 15.67 ± 0.27, and 12.30 ± 1.66 %ID/g at 24, 48, and 72 h, respectively (n = 2).

Moreover, orthotopic BT-474 tumor uptake of ^{64}Cu-NOTA-trastuzumab accumulated and was clearly visible at 6 h, peaked at 51 h, and remained prominent over time (2.48 ± 1.69, 3.08 ± 2.47, 3.53 ± 2.99, and 2.92 ± 3.92 %ID/g at 6, 28, 51, and 122 h, respectively). An autoradiogram of the frozen section prepared from the removed HER2-positive tumor revealed high accumulation in the areas where HER2-positive cells were detected by immunohistochemistry (Fig. 3).

Biodistribution of ^{64}Cu-NOTA-Trastuzumab in HER2-Positive Breast Tumor Model and Normal Mice

Biodistribution data of ^{64}Cu-NOTA-trastuzumab in BT-474 HER2–positive tumor models were compared and are summarized in Figure 4. The ^{64}Cu-NOTA-trastuzumab uptake of major organs and tissues in tumor-bearing mice was similar to that in normal mice. The radioactivity in blood and spleen was high at 2 h but gradually decreased over time. The uptake of ^{64}Cu-NOTA-trastuzumab in BT-474 HER2–positive tumors steadily increased and peaked at 48 h, at 64.44 ± 31.11 %ID/g.

Pharmacokinetics of ^{64}Cu-NOTA-Trastuzumab in Nude Mice With or Without HER2-Positive Tumors

The blood radioactivity concentration–time profiles after a single intravenous bolus injection of ^{64}Cu-NOTA-trastuzumab in nude mice with or without BT-474 tumor xenografts are shown in Figure 5. In both groups of mice, blood radioactivity concentrations decreased biexponentially with time. The concentration–time profiles in tumor-bearing nude mice were similar to those in the nude mice without tumors. Table 1 summarizes the pharmacokinetic parameters obtained by noncompartmental analysis. The blood concentration extrapolated to time zero was 46.8 ± 7.52 and 48.7 ± 4.64 %ID/mL; the terminal elimination half-life was 135 ± 41.1 and 190 ± 40.2 h; the area under the blood concentration–time curve from 0 to 72 h was 1,354 ± 166 and 1,480 ± 124 %ID·h/mL; the volume of distribution at the terminal phase was 4.74 ± 0.786 and 4.69 ± 0.461 mL; the systemic clearance was 0.0254 ± 0.00538 and 0.0176 ± 0.00289 mL/h; and the mean retention time was 31.0 ± 0.512 and 31.6 ± 0.390 h, respectively, after intravenous injection of ^{64}Cu-NOTA-trastuzumab in nude mice with and without tumors.

Residence Time Calculation

To clearly define each organ region, we acquired CT images using a contrast agent. As a result, we clearly defined the region of interest in the PET image data. The segmented tumor and major organs are shown in Figure 6A. The time–activity curve was calculated at each time point (1, 2, and 6 h, and 1, 2, and 3 d) using the defined specific region in the PET image (Fig. 6B). The highest mean residence time was in the tumor, followed by the kidney,

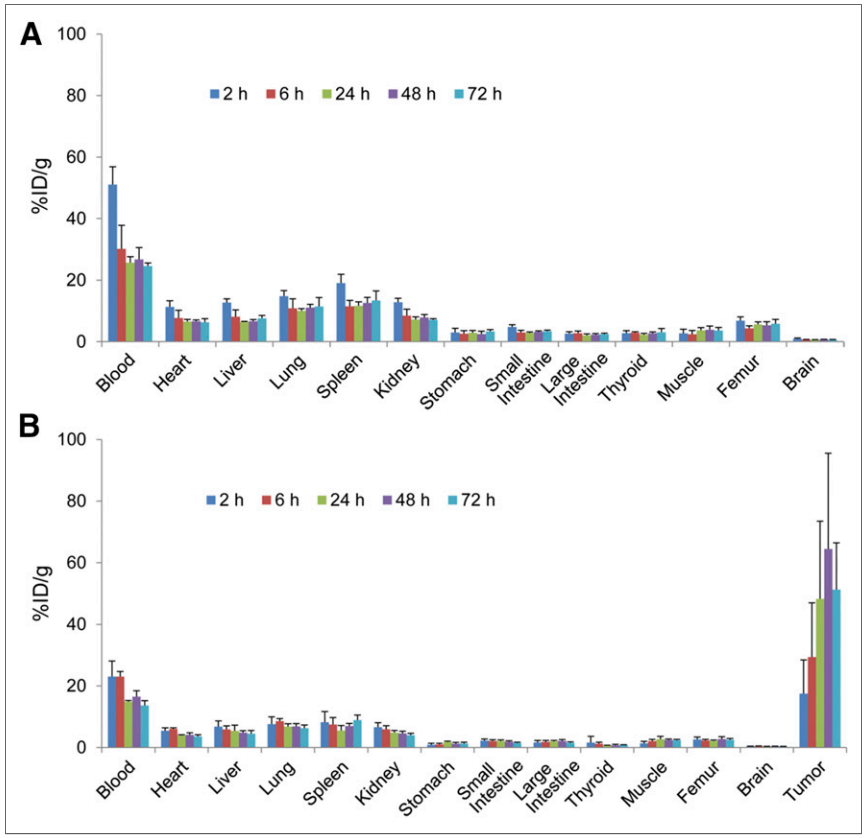

FIGURE 4. Biodistribution of ^{64}Cu-NOTA-trastuzumab in normal mice (A) and HER2-positive tumor–bearing mice (B). At 2, 6, 24, 48, and 72 h after injection of ^{64}Cu-NOTA-trastuzumab, both mice were euthanized, and radioactivity in organs was measured (n = 4).

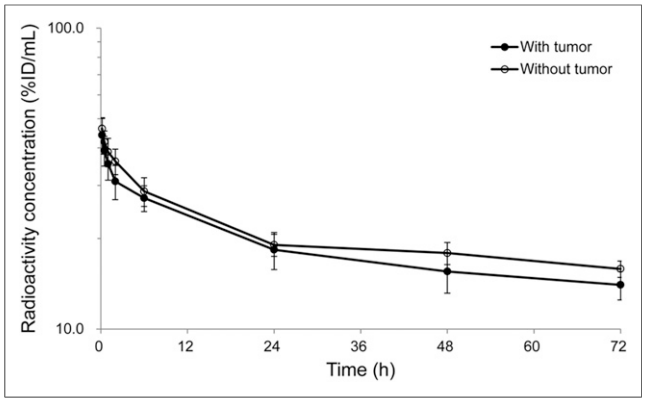

FIGURE 5. Average blood radioactivity concentration vs. time after intravenous injection of ^{64}Cu-NOTA-trastuzumab in nude mice with or without BT-474 tumor xenografts. Data are mean ± SD.

heart, liver, lung, urinary bladder, spleen, and stomach; the lowest residence time was in the brain (Fig. 6C). The mean residence time in the tumors was 7.42 ± 3.3 MBq-h/MBq. The residence time in the heart was 3.33 ± 0.8 MBq-h/MBq. The residence time in the lung was 2.28 ± 0.7 MBq-h/MBq, and that in the liver was 2.66 ± 0.8 MBq-h/MBq. The residence time in the stomach was 1.31 ± 0.2 MBq-h/MBq, and that in the spleen was 2.19 ± 0.6 MBq-h/MBq.

Absorbed Dose Calculation

S value was calculated with both ^{64}Cu and ^{67}Cu using Monte Carlo simulation with the CT images. As shown in Tables 2 and 3, S value was higher with the self-irradiation than with the cross-irradiation and was highest in the HER2-positive tumors, followed by the spleen, brain, urinary bladder, heart, kidney, and liver. We calculated the absorbed dose of ^{64}Cu-NOTA-trastuzumab using an image-based approach. The absorbed dose of ^{64}Cu-NOTA-trastuzumab was 0.048 ± 0.012 for heart, 0.079 ± 0.004 for liver, 0.047 ± 0.010 for spleen, and 2.43 ± 1.09 mGy/MBq for tumor. According to a study by Tamura et al. (*12*), the absorbed dose of ^{64}Cu-DOTA-trastuzumab was 0.34 ± 0.046 for heart, 0.24 ± 0.117 for liver, and 0.14 ± 0.04 mGy/MBq for spleen (Fig. 7). Consequently, the absorbed dose of ^{64}Cu-NOTA-trastuzumab was lower than that of ^{64}Cu-DOTA-trastuzumab in the heart, liver, and spleen. We also calculated the absorbed dose of ^{67}Cu-NOTA-trastuzumab using Monte Carlo simulation to develop ^{67}Cu-NOTA-trastuzumab as a therapeutic agent for HER2-positive breast cancer based on ^{64}Cu-NOTA-trastuzumab. The absorbed doses of ^{67}Cu-NOTA-trastuzumab and ^{67}Cu-DOTA-trastuzumab in liver were 0.042 and 0.934 mGy/MBq, respectively, calculated using the biodistribution results published by Paudyal et al. (*25*). Therefore, ^{67}Cu-NOTA-trastuzumab might be safer than ^{67}Cu-DOTA-trastuzumab because of the lower absorbed dose in major organs such as liver, heart, and spleen.

DISCUSSION

Breast cancer is the most common malignancy. It is a heterogeneous disease that can be classified by microscopic appearance and molecular profiles that include the expression of estrogen receptor and overexpression of HER2 (*3*). Overexpression of HER2 portends a poor prognosis with an increased risk for disease progression and decreased overall survival (*26*).

The discovery of many novel molecular targets for anticancer treatment has led to the development of therapeutic antibodies. Overexpression of HER2 enables constitutive activation of growth factor signaling pathways and thereby serves as an oncogenic driver in breast cancer. Through both genetic and pharmacologic approaches, it was determined that HER2 is both necessary and sufficient for tumor formation and maintenance in models of HER2-positive breast cancer (*27*). Targeting HER2 with monoclonal antibody, such as trastuzumab and pertuzumab, is a well-established therapeutic strategy for HER2-positive breast cancer in neoadjuvant (*28*), adjuvant (*29,30*), and metastatic settings (*31,32*). Especially trastuzumab, a humanized recombinant monoclonal antibody against HER2, is widely used as a standard treatment for HER2-expressing breast cancer. Recently, a need has been recognized for repetitive visualization of HER2 expression due to the success of trastuzumab–emtansine as an antibody–drug conjugate to minimize toxicity against major organs and enhance therapeutic efficacy. Detection of HER2-positive metastatic tumors using radiolabeled HER2 antibodies would be valuable to provide safety, treatment economy, and other therapeutic options to HER2-negative tumor–bearing patients. Conversely, Ulaner et al. reported that ^{89}Zr-labeled trastuzumab PET/CT could be applied to detect unsuspected HER2-positive metastases in patients with HER2-negative primary breast cancer as a proof-of-concept

TABLE 1
Blood Radioactivity Parameters After ^{64}Cu-NOTA-Trastuzumab* in Mice With and Without BT-474 Tumors

Parameter	With tumor	Without tumor	*P*
C_0 (%ID/mL)	46.8 ± 7.52	48.7 ± 4.64	0.605
$t_{1/2,\lambda z}$ (h)	135 ± 41.1	190 ± 40.2	0.041
$AUC_{0-72\ h}$ (%ID·h/mL)	1,354 ± 166	1,480 ± 124	0.167
V_z (mL)	4.74 ± 0.786	4.69 ± 0.461	0.892
Cl (mL/h)	0.0254 ± 0.00538	0.0176 ± 0.00289	0.011
Last MRT (h)	31.0 ± 0.512	31.6 ± 0.390	0.051

*Dose, 100 μg/150–180 μCi/head.

C_0 = blood concentration extrapolated to time zero; $t_{1/2,\lambda z}$ = terminal elimination half-life; $AUC_{0-72\ h}$ = area under blood concentration–time curve from 0 to 72 h; V_z = volume of distribution at terminal phase; Cl = systemic clearance; MRT = mean retention time.

Data are mean ± SD.

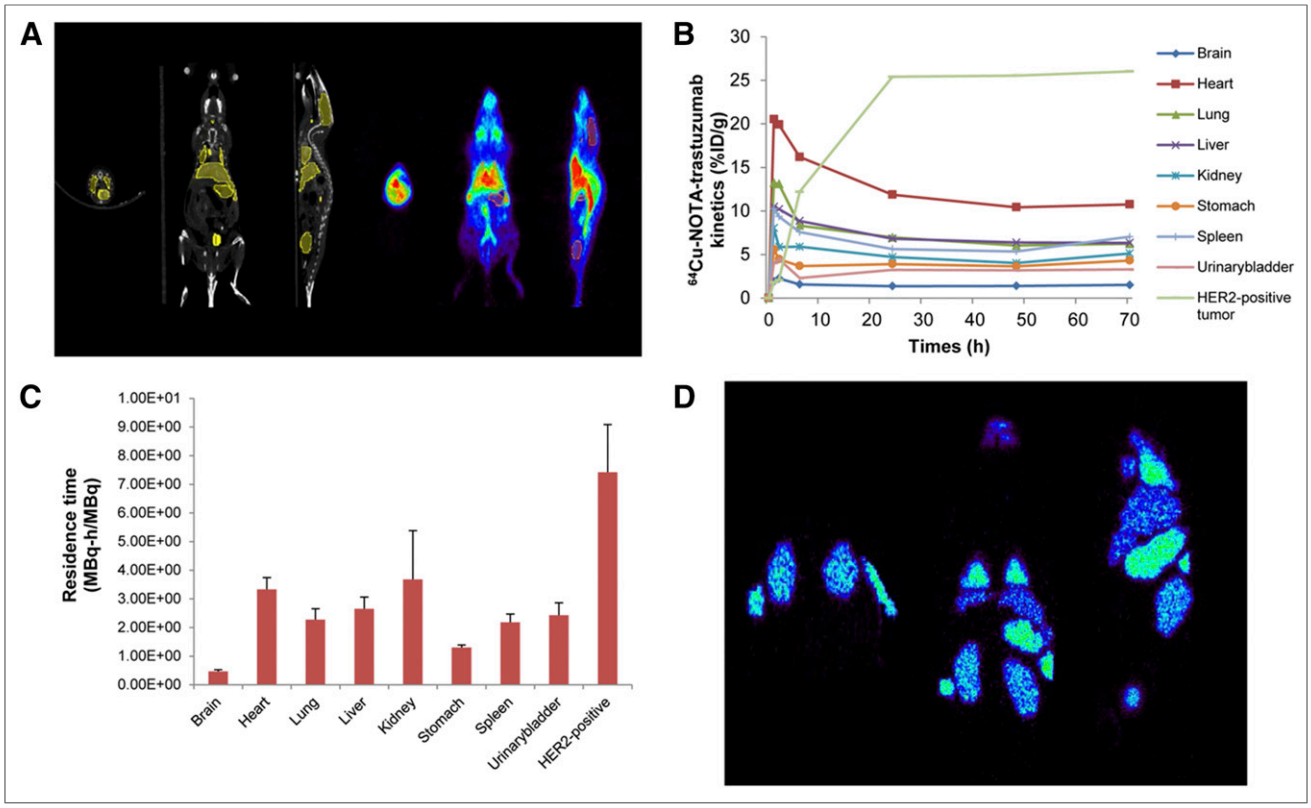

FIGURE 6. (A) Acquired CT and PET images. (B) Time–activity curve evaluated by segmented PET image data at 6 time points. (C) Calculated residence time in each organ and tumor. (D) Energy map generated from Monte Carlo simulation.

clinical study (*32*). Thus, it is important to evaluate HER2 expression in metastatic and primary tumors to determine whether anti-HER2 therapy is indicated.

Although HER2 expression is routinely determined using histologic analysis (*33*), technical problems can arise when lesions cannot be easily accessed by core-needle biopsy, and the analysis lacks specificity and sensitivity (*34*). In addition, HER2 expression can vary during the course of the disease and even across tumor lesions within the same patient. To overcome these problems, novel techniques such as PET and SPECT have been studied for evaluating HER2 expression. Molecular imaging using radiolabeled antibodies can provide real-time information and noninvasively assess the presence of specific targets throughout the body (*35*). PET imaging depends on the delivery of a targeting ligand containing a positron-emitting radionuclide to a tissue or organ of interest. ^{64}Cu (half-life, 12.7 h) is an attractive radionuclide for PET imaging that can be used for both diagnostic imaging and radionuclide therapy because of its dual decay characteristics (*36*). PET images acquired by ^{64}Cu-labeled trastuzumab may potentially achieve good contrast with high resolution and low radiation exposure because of the shorter half-life of the radioisotope (*12*). However, the application of ^{64}Cu as a radioisotope for antibody molecules has been hindered

TABLE 2
^{64}Cu S Values Calculated Using Monte Carlo Simulation with CT Image

Site	Brain	Heart	Lung	Liver	Kidney	Stomach	Spleen	Bladder	Tumor
Brain	1.87E−01	3.39E−05	2.34E−05	9.14E−06	4.02E−06	8.93E−06	4.71E−06	1.38E−06	4.00E−06
Heart	2.41E−05	1.05E−01	1.13E−03	1.97E−04	1.64E−05	4.17E−05	2.29E−05	4.30E−06	1.08E−05
Lung	2.23E−05	1.07E−03	1.32E−01	5.70E−04	3.23E−05	5.28E−05	2.86E−05	7.40E−06	1.86E−05
Liver	1.26E−05	2.08E−04	5.90E−04	2.12E−02	4.49E−05	5.56E−04	3.33E−04	1.23E−05	2.89E−05
Kidney	4.51E−06	2.16E−05	2.80E−05	4.06E−05	6.77E−02	1.08E−04	1.63E−04	2.55E−05	3.06E−04
Stomach	4.95E−06	3.97E−05	4.56E−05	5.67E−04	9.71E−05	6.92E−02	8.32E−04	2.02E−05	2.47E−05
Spleen	4.56E−06	1.74E−05	2.51E−05	3.30E−04	1.43E−04	8.22E−04	2.43E−01	2.24E−05	2.06E−05
Bladder	1.78E−06	6.84E−06	6.93E−06	1.07E−05	2.58E−05	2.26E−05	1.89E−05	1.13E−01	1.85E−05
Tumor	9.09E−06	2.65E−05	3.20E−05	5.90E−05	4.59E−04	4.74E−05	3.11E−05	4.61E−05	3.28E−01

TABLE 3
^{67}Cu S Values Calculated Using Monte Carlo Simulation with CT Image

Site	Brain	Heart	Lung	Liver	Kidney	Stomach	Spleen	Bladder	Tumor
Brain	8.54E−02	1.30E−05	1.18E−05	6.75E−06	5.01E−06	4.97E−06	2.61E−06	1.31E−06	4.41E−06
Heart	1.23E−05	1.38E−01	4.79E−04	1.49E−04	1.19E−05	2.43E−05	9.16E−06	4.70E−06	1.21E−05
Lung	1.22E−05	5.17E−04	1.79E−01	5.47E−04	1.56E−05	2.46E−05	1.66E−05	4.74E−06	1.81E−05
Liver	8.11E−06	1.45E−04	5.02E−04	2.76E−02	2.43E−05	4.04E−04	2.13E−04	6.01E−06	2.57E−05
Kidney	4.46E−06	1.31E−05	1.45E−05	2.67E−05	8.33E−02	5.66E−05	1.02E−04	1.83E−05	2.81E−04
Stomach	5.35E−06	2.22E−05	2.42E−05	4.11E−04	5.88E−05	8.54E−02	3.14E−04	1.07E−05	2.35E−05
Spleen	4.15E−06	1.31E−05	1.38E−05	2.09E−04	1.00E−04	3.23E−04	3.07E−01	1.30E−05	1.69E−05
Bladder	1.80E−06	5.20E−06	3.45E−06	6.35E−06	1.74E−05	1.11E−05	1.35E−05	1.30E−01	1.70E−05
Tumor	3.03E−06	9.70E−06	1.04E−05	1.57E−05	1.80E−04	1.59E−05	1.17E−05	1.33E−05	4.01E−01

by the lack of an optimal chelator to form a stable conjugate complex in vivo. The high uptake and retention of copper-containing compounds in the blood and liver are well known (*37,38*). Therefore, an optimal chelator for copper metal ion for a more stable conjugate is required for in vivo studies using ^{64}Cu. NOTA is an intensively investigated macrocyclic, multidentate chelator used for complexation of a broad variety of bi- and trivalent metal ions (*39–41*). Bifunctional NOTA forms an exceedingly stable complex with Ga^{3+} ions, and PET agents can feature its use. NOTA conjugates labeled with ^{67}Ga, ^{68}Ga, ^{64}Cu, ^{67}Cu, and ^{111}In are suitable for diagnostic and therapeutic approaches (*42,43*). According to a report of Paudyal et al. (*25*), uptake of ^{64}Cu-DOTA-trastuzumab in liver was 26.9 ± 7.4 %ID/g at 24 h. In contrast, uptake of ^{64}Cu-NOTA-trastuzumab in liver was 5.44 ± 1.84 %ID/g at 24 h (Fig. 4). This result suggests that release of ^{64}Cu from ^{64}Cu-NOTA-trastuzumab is less than that from ^{64}Cu-DOTA-trastuzumab and, therefore, that ^{64}Cu-NOTA-trastuzumab is more stable than ^{64}Cu-DOTA-trastuzumab.

According to the pharmacokinetic results of ^{64}Cu-NOTA-trastuzumab in HER2-positive tumor–bearing and non–tumor-bearing nude mice, the systemic clearance and terminal half-life were significantly different from each other ($P < 0.05$; Fig. 5), whereas other parameters were quite similar to each other. The systemic clearance in nude mice with HER2-positive tumors was higher than that in nude mice without tumors. This result suggests that the elimination rate of ^{64}Cu-NOTA-trastuzumab in nude mice with HER2-positive tumors is faster than that in nude mice without tumors and that this might be because ^{64}Cu-NOTA-trastuzumab is targeted, trapped to HER2-positive tumors, and removed from mouse circulation.

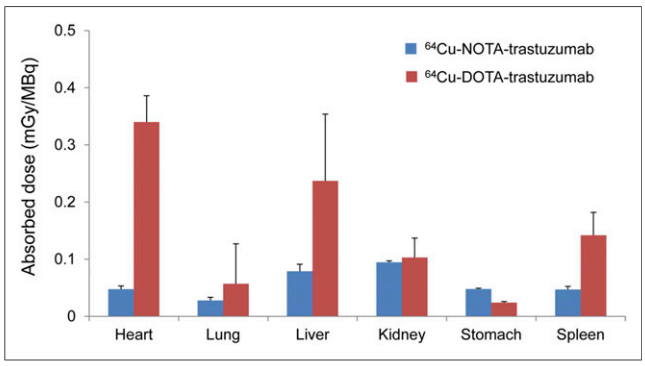

FIGURE 7. ^{64}Cu-DOTA-trastuzumab exhibited higher absorbed dose than ^{64}Cu-NOTA-trastuzumab in heart, liver, and spleen (*12*).

The image-based methods basically include Monte Carlo simulation and entail manually drawing regions of interest to calculate the individual specific dosimetry based on the patient's anatomic image. Monte Carlo simulation can be used for acquiring the S values of different radionuclides. If the same pharmacokinetic or pharmacodynamic characteristics exist between a diagnostic radiopharmaceutical, such as emitting γ-rays, and a therapeutic radiopharmaceutical, such as emitting α- or β-particles, it may be possible to calculate the subject-specific internal dosimetry using the diagnostic radiopharmaceutical (*44*). To develop ^{67}Cu-NOTA-trastuzumab as a therapeutic agent based on ^{64}Cu-NOTA-trastuzumab, we calculated the absorbed dose of ^{67}Cu-NOTA-trastuzumab in this study using Monte Carlo simulation. The lower absorbed dose of ^{67}Cu-NOTA-trastuzumab in major organs showed it to have greater safety than ^{67}Cu-DOTA-trastuzumab. Therefore, NOTA-conjugated trastuzumab might be suitable for both therapeutic and PET-diagnostic applications in HER2-positive breast cancer.

CONCLUSION

Trastuzumab as a HER2-targeting antibody can be efficiently radiolabeled with ^{64}Cu using NOTA as a chelator with high labeling yield and excellent stability. The calculated absorbed dose of ^{64}Cu-NOTA-trastuzumab was lower than that of ^{64}Cu-DOTA-trastuzumab in heart, liver, and spleen because of a short residence time. Furthermore, ^{64}Cu-NOTA-trastuzumab was efficiently targeted to the HER2-expressing tumors in vivo and in vitro. Therefore, ^{64}Cu-NOTA-trastuzumab might be applicable in human studies for selecting patients with the right timing for HER2 therapy and for monitoring the response after HER2-targeted therapy.

DISCLOSURE

This work was supported by National Research Foundation of Korea (NRF) grants funded by the Ministry of Science and ICT (NRF-2012M2A2A7013480, NRF-2015R1C1A1A02036885, and NRF-2017M2A2A02070985). No other potential conflict of interest relevant to this article was reported.

REFERENCES

1. Okines AF, Cunningham D. Trastuzumab in gastric cancer. *Eur J Cancer.* 2010;46: 1949–1959.
2. Schrama D, Reisfeld RA, Becker JC. Antibody targeted drugs as cancer therapeutics. *Nat Rev Drug Discov.* 2006;5:147–159.
3. Slamon DJ, Clark GM, Wong SG, et al. Human breast cancer: correlation of relapse and survival with amplification of the HER-2/neu oncogene. *Science.* 1987; 235:177–182.
4. Loibl S, Gianni L. HER2-positive breast cancer. *Lancet.* 2017;389:2415–2429.
5. Jiang H, Rugo HS. Human epidermal growth factor receptor 2 positive (HER2+) metastatic breast cancer: how the latest results are improving therapeutic options. *Ther Adv Med Oncol.* 2015;7:321–339.
6. Gebhart G, Flamen P, De Vries EG, et al. Imaging diagnostic and therapeutic targets: human epidermal growth factor receptor 2. *J Nucl Med.* 2016;57(suppl): 81S–88S.
7. Niu G, Li Z, Cao Q, et al. Monitoring therapeutic response of human ovarian cancer to 17-DMAG by noninvasive PET imaging with ^{64}Cu-DOTA-trastuzumab. *Eur J Nucl Med Mol Imaging.* 2009;36:1510–1519.
8. Orlova A, Wållberg H, Stone-Elander S, et al. On the selection of a tracer for PET imaging of HER2-expressing tumors: direct comparison of a ^{124}I-labeled affibody molecule and trastuzumab in a murine xenograft model. *J Nucl Med.* 2009;50:417–425.
9. Perik PJ, Lub-De Hooge MN, Gietema JA, et al. Indium-111-labeled trastuzumab scintigraphy in patients with human epidermal growth factor receptor 2-positive metastatic breast cancer. *J Clin Oncol.* 2006;24:2276–2282.
10. Dijkers EC, Kosterink JG, Rademaker AP, et al. Development and characterization of clinical-grade ^{89}Zr-trastuzumab for HER2/neu immunoPET imaging. *J Nucl Med.* 2009;50:974–981.
11. Kurihara H, Hamada A, Yoshida M, et al. ^{64}Cu-DOTA-trastuzumab PET imaging and HER2 specificity of brain metastases in HER2-positive breast cancer patients. *EJNMMI Res.* 2015;5:8.
12. Tamura K, Kurihara H, Yonemori K, et al. ^{64}Cu-DOTA-trastuzumab PET imaging in patients with HER2-positive breast cancer. *J Nucl Med.* 2013;54:1869–1875.
13. Mortimer JE, Bading JR, Colcher DM, et al. Functional imaging of human epidermal growth factor receptor 2-positive metastatic breast cancer using ^{64}Cu-DOTA-trastuzumab PET. *J Nucl Med.* 2014;55:23–29.
14. Mortimer JE, Bading JR, Park JM, et al. Tumor uptake of ^{64}Cu-DOTA-trastuzumab in patients with metastatic breast cancer. *J Nucl Med.* 2018;59:38–43.
15. Kristensen L, Nielsen C, Nedergaard M, et al. ^{64}Cu-DOTA-trastuzumab imaging in a HER2-positive intracranial patient-derived xenograft (PDX) model of breast cancer metastasis [abstract]. *J Nucl Med.* 2016;57(suppl 2):1338.
16. Rizzieri D. Zevalin® (ibritumomab tiuxetan): after more than a decade of treatment experience, what have we learned? *Crit Rev Oncol Hematol.* 2016;105: 5–17.
17. Kim KI, Jang SJ, Park JH, et al. Detection of increased ^{64}Cu uptake by human copper transporter 1 gene overexpression using PET with $^{64}CuCl_2$ in human breast cancer xenograft model. *J Nucl Med.* 2014;55:1692–1698.
18. Kraeber-Bodéré F, Rousseau C, Bodet-Milin C, et al. Tumor immunotargeting using innovative radionuclides. *Int J Mol Sci.* 2015;16:3932–3954.
19. Prasanphanich AF, Nanda PK, Rold TL, et al. [^{64}Cu-NOTA-8-Aoc-BBN(7-14)NH_2] targeting vector for positron-emission tomography imaging of gastrin releasing peptide receptor-expressing tissues. *Proc Natl Acad Sci USA.* 2007;104: 12462–12467.
20. Bouchet LG, Bolch WE, Blanco HP, et al. MIRD pamphlet no. 19: absorbed fractions and radionuclide S values for six age-dependent multiregion models of the kidney. *J Nucl Med.* 2003;44:1113–1147.
21. Park YS, Lee YJ, Kim W, et al. Image-based absorbed dosimetry of radioisotope. *Prog Med Phys.* 2016;27:86–91.
22. Kim JY, Park H, Lee JC, et al. A simple Cu-64 production and its application of Cu-64 ATSM. *Appl Radiat Isot.* 2009;67:1190–1194.
23. Lindmo T, Boven E, Cuttitta F, et al. Determination of the immunoreactive function of radiolabeled monoclonal antibodies by linear extrapolation to binding at infinite antigen excess. *J Immunol Methods.* 1984;72:77–89.
24. Snyder W, Ford MR, Warner G, et al. *MIRD Pamphlet No. 11: "S," Absorbed Dose per Unit Cumulated Activity for Selected Radionuclides and Organs.* Reston, VA: Society of Nuclear Medicine and Molecular Imaging; 1975:5–257.
25. Paudyal P, Paudyal B, Hanaoka H, et al. Imaging and biodistribution of Her2/neu expression in non-small cell lung cancer xenografts with ^{64}Cu-labeled trastuzumab PET. *Cancer Sci.* 2010;101:1045–1050.
26. Sjögren S, Inganäs M, Lindgren A, et al. Prognostic and predictive value of c-erbB-2 overexpression in primary breast cancer, alone and in combination with other prognostic markers. *J Clin Oncol.* 1998;16:462–469.
27. Buzdar AU, Ibrahim NK, Francis D, et al. Significantly higher pathologic complete remission rate after neoadjuvant therapy with trastuzumab, paclitaxel, and epirubicin chemotherapy: results of a randomized trial in human epidermal growth factor receptor 2–positive operable breast cancer. *J Clin Oncol.* 2005;23:3676–3685.
28. Piccart-Gebhart MJ, Procter M, Leyland-Jones B, et al. Trastuzumab after adjuvant chemotherapy in HER2-positive breast cancer. *N Engl J Med.* 2005;353: 1659–1672.
29. Romond EH, Perez EA, Bryant J, et al. Trastuzumab plus adjuvant chemotherapy for operable HER2-positive breast cancer. *N Engl J Med.* 2005;353:1673–1684.
30. Slamon DJ, Leyland-Jones B, Shak S, et al. Use of chemotherapy plus a monoclonal antibody against HER2 for metastatic breast cancer that overexpresses HER2. *N Engl J Med.* 2001;344:783–792.
31. Tripathy D, Slamon DJ, Cobleigh M, et al. Safety of treatment of metastatic breast cancer with trastuzumab beyond disease progression. *J Clin Oncol.* 2004;22: 1063–1070.
32. Ulaner GA, Hyman DM, Lyashchenko SK, et al. ^{89}Zr-trastuzumab PET/CT for detection of human epidermal growth factor receptor 2–positive metastases in patients with human epidermal growth factor receptor 2–negative primary breast cancer. *Clin Nucl Med.* 2017;42:912–917.
33. Sauter G, Lee J, Bartlett JM, et al. Guidelines for human epidermal growth factor receptor 2 testing: biologic and methodologic considerations. *J Clin Oncol.* 2009; 27:1323–1333.
34. Lebeau A, Turzynski A, Braun S, et al. Reliability of human epidermal growth factor receptor 2 immunohistochemistry in breast core needle biopsies. *J Clin Oncol.* 2010;28:3264–3270.
35. Song IH, Lee TS, Park YS, et al. Immuno-PET imaging and radioimmunotherapy of ^{64}Cu-/^{177}Lu-labeled anti-EGFR antibody in esophageal squamous cell carcinoma model. *J Nucl Med.* 2016;57:1105–1111.
36. Wadas TJ, Wong E, Weisman G, et al. Copper chelation chemistry and its role in copper radiopharmaceuticals. *Curr Pharm Des.* 2007;13:3–16.
37. Bearn AG, Kunkel HG. Localization of ^{64}Cu in serum fractions following oral administration: an alteration in Wilson's disease. *Proc Soc Exp Biol Med.* 1954;85:44–48.
38. Owen CA, Hazelrig JB. Metabolism of ^{64}Cu-labeled copper by the isolated rat liver. *Am J Physiol.* 1966;210:1059–1064.
39. Wieghardt K, Bossek U, Chaudhuri P, et al. 1,4,7-triazacyclononane-*N,N′,N″*-triacetate (TCTA), a new hexadentate ligand for divalent and trivalent metal ions: crystal structures of [Cr^{III}(TCTA)], [Fe^{III}(TCTA)], and Na[Cu^{II}(TCTA)]·2NaBr·8H_2O. *Inorg Chem.* 1982;21:4308–4314.
40. Cacheris W, Nickle S, Sherry A. Thermodynamic study of lanthanide complexes of 1,4,7-triazacyclononane-N,N′,N″-triacetic acid and 1,4,7,10-tetraazacyclododecane-N,N′,N″,N‴-tetraacetic acid. *Inorg Chem.* 1987;26:958–960.
41. Boeyens JC, van der Merwe MJ. The nonexistent crystals of macrocyclic nickel (III): structure of the cobalt (III) complex of 1, 4, 7-triazacyclononane-N,N′,N″-triacetate. *Inorg Chem.* 1997;36:3779–3780.
42. Roosenburg S, Laverman P, Joosten L, et al. PET and SPECT imaging of a radiolabeled minigastrin analogue conjugated with DOTA, NOTA, and NODAGA and labeled with ^{64}Cu, ^{68}Ga, and ^{111}In. *Mol Pharm.* 2014;11:3930–3937.
43. Guleria M, Das T, Amirdhanayagam J, et al. Comparative evaluation of using NOTA and DOTA derivatives as bifunctional chelating agents in the preparation of ^{68}Ga-labeled porphyrin: impact on pharmacokinetics and tumor uptake in a mouse model. *Cancer Biother Radiopharm.* 2018;33:8–16.
44. Huang S-Y, Bolch WE, Lee C, et al. Patient-specific dosimetry using pretherapy [^{124}I]m-iodobenzylguanidine ([^{124}I]mIBG) dynamic PET/CT imaging before [^{131}I]mIBG targeted radionuclide therapy for neuroblastoma. *Mol Imaging Biol.* 2015;17:284–294.